CHAPTER 5

INVESTIGATIONS ON THE DUAL SEGMENT CYLINDRICAL DIELECTRIC RESONATOR ANTENNA (DS–CDRA) ON LMAP–LTCC SUBSTRATE

5.1 Introduction

Ceramic materials find application as substrates in integrated circuits, thermally stable resonators, filters, oscillators, phase shifters, isolators, circulators and dielectric resonator antennas in microwave and millimetre wave communication and radar systems. Low dielectric constant, low loss tangent and good thermal stability are primary requirements for substrate materials to achieve efficient signal transmission. Low loss ceramic materials used in the circuit improve its performance by reducing the power dissipation and the insertion loss, which suppresses the electrical noise in oscillators and can produce highly selective filters and low loss phase shifters [Sebastian and Jantunen (2008b)]. Further, by selecting a low loss ceramic material for realizing a dielectric resonator antenna (DRA), the radiation efficiency can be enhanced due to low conductor and dielectric losses as well as absence of surface waves associated with DRA. Different manufacturers produce similar components for specific applications, however, there are subtle differences in their circuit designs, construction and packaging.

This chapter describes the study of a Dual segment cylindrical dielectric resonator antenna (DS–CDRA) designed using the prepared Li_2O–1.94MgO–0.02Al_2O_3–P_2O_5 (LMAP) ceramic material as substrate. The simulation study on the proposed antenna was performed using Ansys HFSS software and the simulation results for the DS–CDRA are compared with the respective measured results.

5.2 Material description

The CDRA is characterized by its height, radius and material dielectric constant. For the design of a microstrip fed aperture couple DS–CDRA antenna, Li_2O–1.94MgO–$0.02Al_2O_3$–P_2O_5 ceramic having maximum density when compared with the other compositions (Chapter 4) is used as a substrate material with $\varepsilon_r = 6.2$ and $\tan\delta = 0.0006$. Silver coating was done on the substrate for making the conductive ground plane and the microstrip line for excitation of antenna through slot coupling. Upper segment of the proposed DS–CDRA is made of high dielectric constant ceramic material i.e PbO–BaO–B_2O_3–SiO_2 glass added Barium Strontium Titanate (BSTG with $\varepsilon_r = 27$ and $\tan\delta = 0.121$) and lower segment is of low dielectric constant material (Teflon with $\varepsilon_r = 2.1$ and $\tan\delta = 0.001$). The procedure for material preparation is described in detail in Chapter 3 (Section 3.1).

5.3 Antenna design and fabrication

The simulation study of a DS–CDRA designed on LMAP LTCC (Low Temperature co-fired ceramic) substrate for X– band application is described. The simulation study was performed using Ansys HFSS software. The geometry of the proposed antenna is shown in Figure 5.1. The LMAP ceramic ($\varepsilon_r = 6.2$ and $\tan\delta = 0.0006$) having dimensions 40 mm × 40 mm × 1.2 mm is taken as substrate (Figure 5.2(a)). Steps involved for the coating of silver on the ceramic substrate is described in section 3.4.1 of Chapter 3. Top surface of the substrate except the aperture is silver coated which is acting as a conducting ground plane. An aperture of length 8 mm and width 0.9 mm at the centre of the conducting ground plane is shown in Figure 5.2(b). The antenna structure having two dielectric cylindrical segments is placed in the central region of the conducting ground plane above the aperture as shown in Figure 5.1(a). The stacking of the two cylindrical dielectric segments, each having 12 mm of diameter, is done as shown in Figure 5.1(b). The heights

of the lower segment (made of Teflon having $\varepsilon_r = 2.1$ and $\tan\delta = 0.001$) and the upper segment (made of BSTG having $\varepsilon_r = 27$ and $\tan\delta = 0.121$) is 2 mm and 1mm, respectively. The active pattern corresponding to the 50 Ω microstrip feedline of length 25 mm and width 1.6 mm, is printed at the bottom side of the substrate, perpendicular to the length (or larger dimension) of the slot as shown in Figure 5.1(a). To excite the DS–CDRA, aperture coupling was used. The size of the aperture (slot) and extension of microstrip line beyond the slot which is about one quarter guide wavelength were optimized through simulation. All the optimized antenna parameters are given in Table 5.1. Aperture coupling prevents the slot from the spurious feed radiation since the slot gets isolated from the microstrip feed network located below the ground plane. The most common method for exciting the CDRA is the probe or coaxial feed method. However, aperture coupling is selected in order to get the advantage of less spurious feed radiation, large bandwidth and ease of fabrication [Petosa (2007)]. The top and bottom views of the fabricated prototype are shown in Figure 5.2(c) and 5.2(d), respectively.

Table 5.1 Optimized antenna parameters of proposed DS–CDRA.

Parameters	**Dimensions (mm)**
Substrate side length, *sub_L*	40
Substrate thickness, *sub_h*	1.2
Slot length, *Ls*	8
Slot width, *Ws*	0.9
Radius, *R*	6
Stripline width, *Sp_w*	1.6
Stripline length, *Sp_L*	25
BSTG height, *Dr_h*	1
Teflon height, *T_h*	2

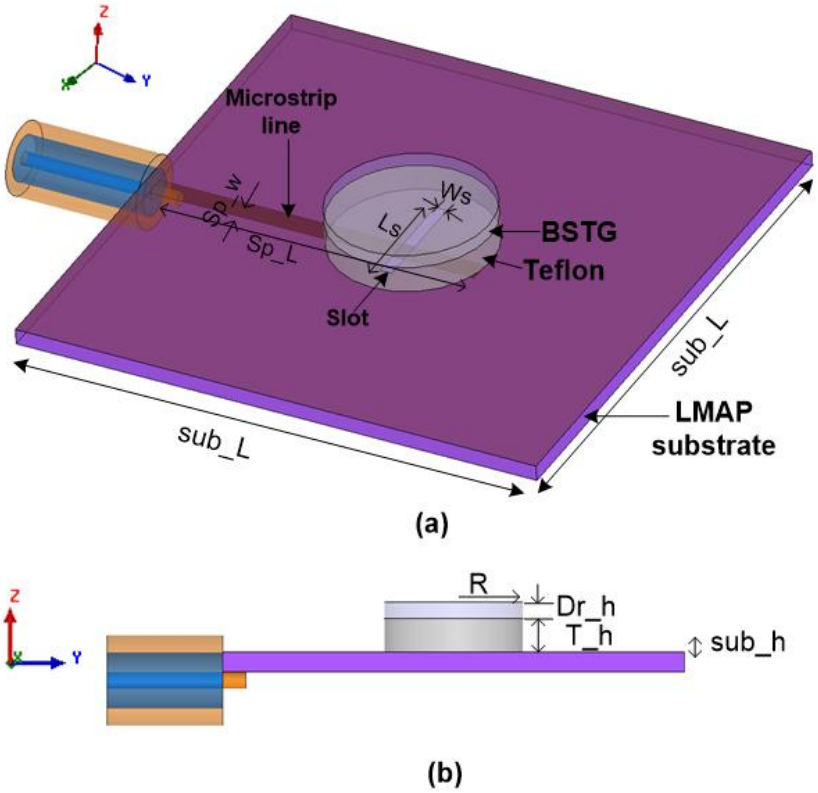

Figure 5.1 Geometry of proposed antenna (a) 3D view and (b) side view.

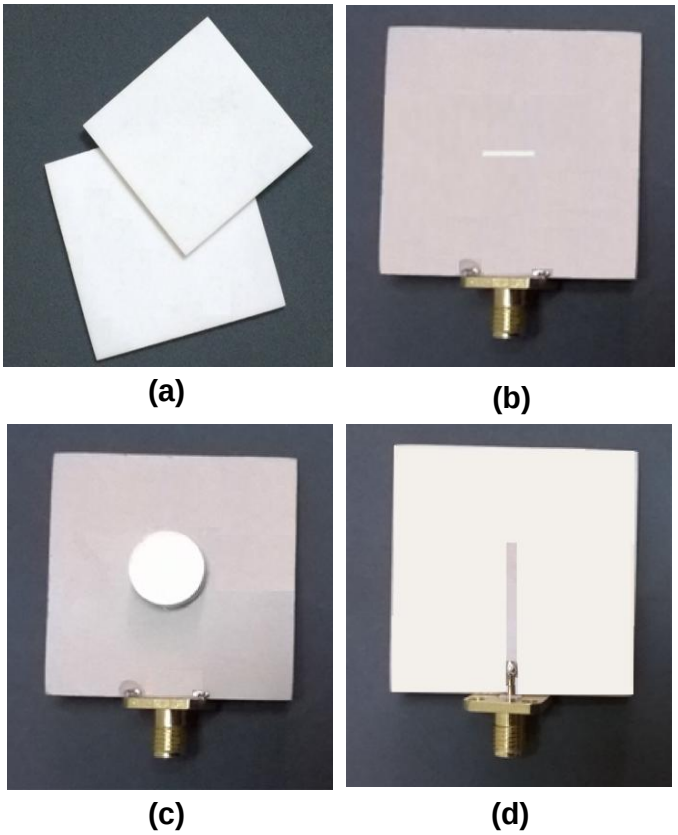

Figure 5.2 (a) Substrate image, (b) slot on fabricated antenna, (c) top view and (d) bottom view of the fabricated antenna.

5.4 Results and discussion

5.4.1 Parametric Study: Reflection coefficient frequency characteristics

The reflection coefficient – frequency characteristics of the proposed DS–CDRA for different slot size were simulated and the results are shown in Figure 5.3. It can be observed from Figure 5.3 that as the slot length increases, the resonant frequency decreases. The optimized slot length '*Ls*' and width '*Ws*' are found to be 0.8 mm and 0.9 mm respectively, corresponding to minimum input reflection coefficient value of -53 dB at the resonant frequency of 9.49 GHz. From the simulation results, it was observed that the -10dB reflection coefficient bandwidth of 910 MHz (9.07 – 9.98 GHz) is achieved with resonant frequency of 9.49 GHz for optimized slot size.

The experimental set-up for the input and radiation characteristics measurement is shown in figure 5.5 and 5.6, respectively. The steps involved for the experimental measurement of the fabricated antenna is described in detail in section 3.5.2 of Chapter 3. The reflection coefficient – frequency characteristics of the fabricated antenna of the optimized dimensions were measured and the measurement results are shown in Figure 5.4. It shows that measured input characteristic of the proposed antenna is nearly in agreement with the simulated characteristic. The measured -10 dB reflection coefficient bandwidth of the proposed antenna is found to be 1080 MHz (8.68 – 9.76 GHz) with resonant frequency of 9.36 GHz.

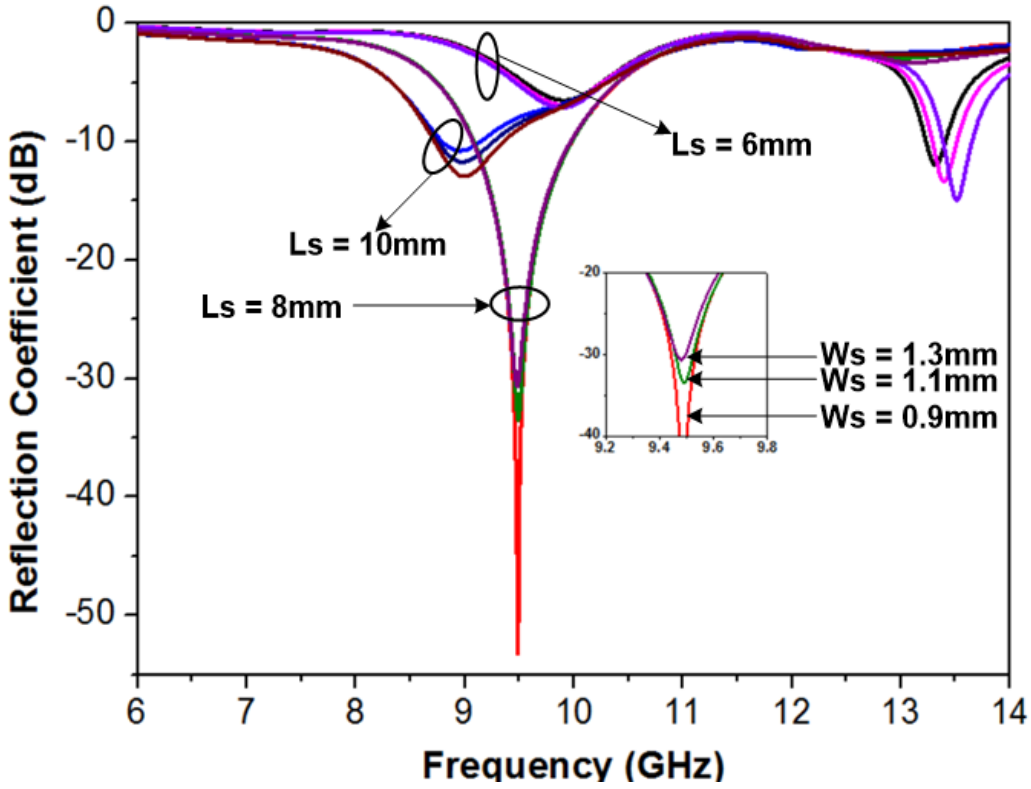

Figure 5.3 Simulated reflection coefficient – frequency characteristics of the proposed DS–CDRA for different slot length and width combinations.

Table 5.2 Slot dimensions optimized from simulation study

***Ls* (mm)**	***Ws* (mm)**	**Operating Bandwidth (GHz)**	**Bandwidth (%)**
6	0.9	13.23 – 13.41	1.35
8	**0.9**	**9.08 – 9.98**	**9.55**
10	0.9	8.79 – 9.15	4.01
6	1.1	13.29 – 13.51	1.64
8	1.1	9.07 – 9.98	9.44
10	1.1	8.75 – 9.25	5.55
6	1.3	13.38 – 13.66	2.07
8	1.3	9.07 – 9.97	9.45
10	1.3	8.72 – 9.35	6.97

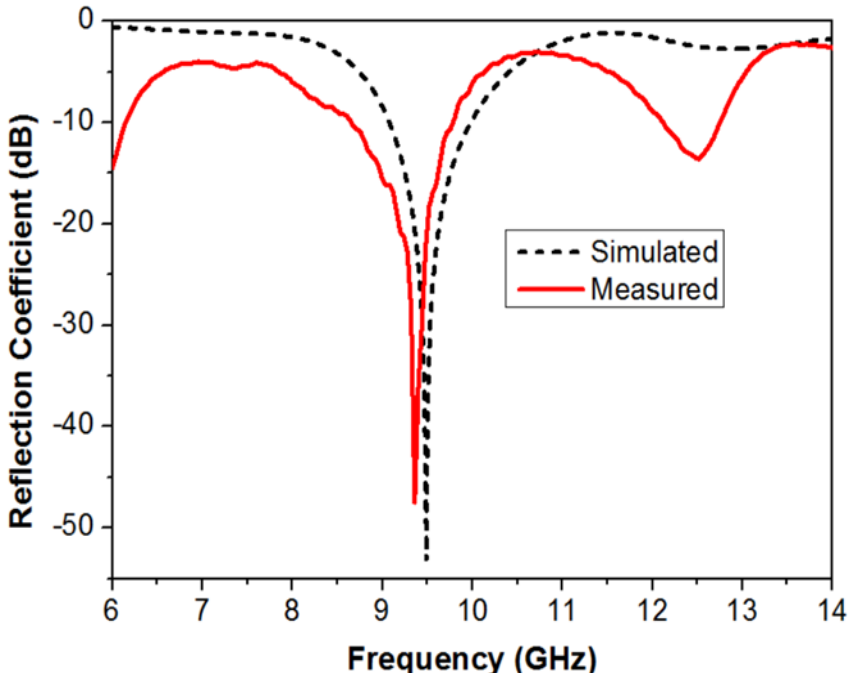

Figure 5.4 Simulated and measured reflection coefficient – frequency characteristics of the proposed DS–CDRA for optimized slot dimensions.

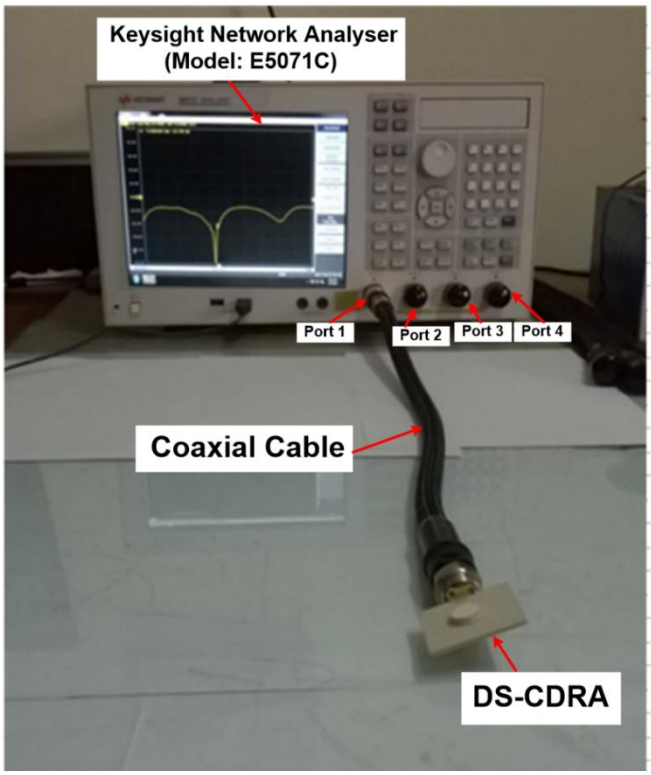

Figure 5.5 Experimental set–up for –10 dB reflection coefficient – frequency measurement.

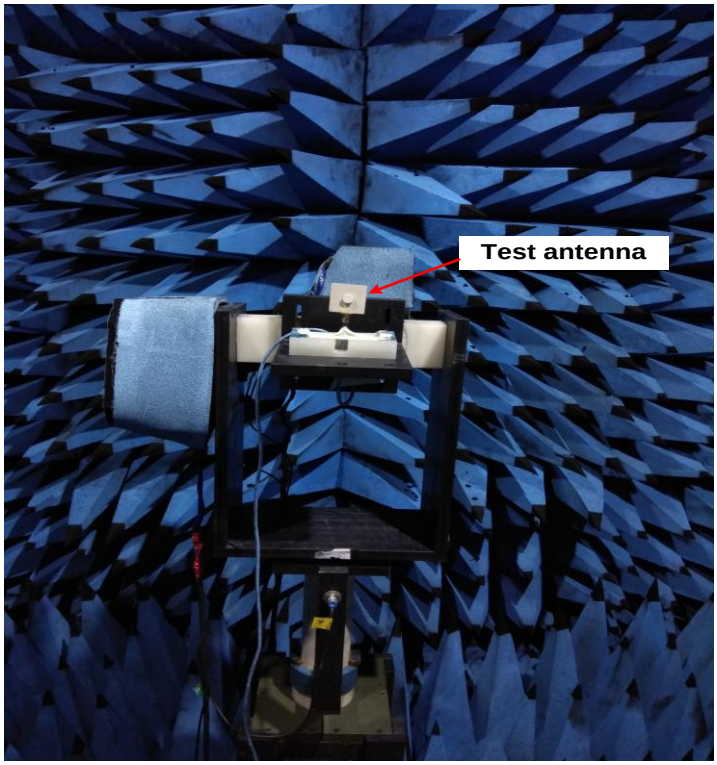

Figure 5.6 Experimental set–up for radiation characteristics measurement of DS–CDRA.

5.4.2 Near field distributions

From the E-field distribution within the DRA of the antenna, it is confirmed that the generated mode within the DRA at its resonant frequency is predominantly the HEM_{11} mode. The excitation of HEM_{11} mode within the CDRA provides broadside radiation pattern. Figure 5.7 shows the E– field distributions in the DS–CDRA at different frequencies.

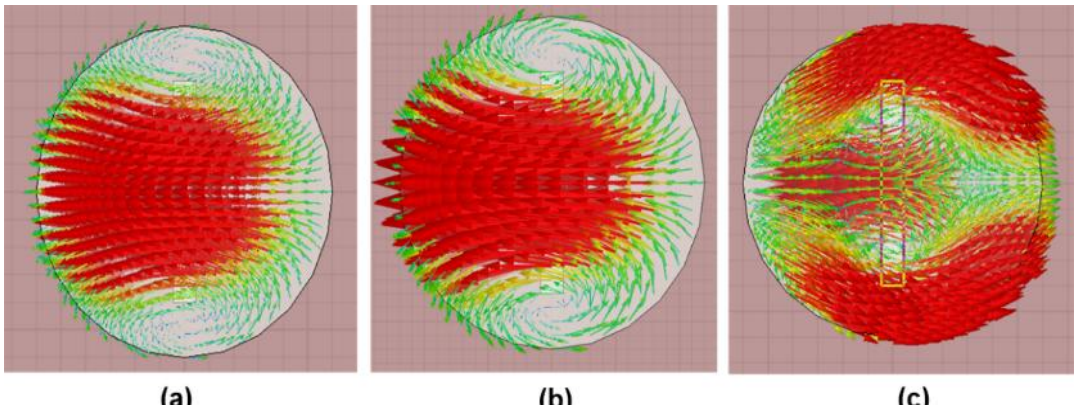

Figure 5.7 E– Field distributions on the upper surface of the DS–CDRA at (a) 9.49 GHz, (b) 9.65 GHz and (c) 9.98 GHz.

5.4.3 Radiation patterns and gain

The co– and cross– polar radiation patterns (2D) of the proposed antenna in E– and H–plane at 9.36 GHz are shown in Figure 5.8, whereas realized gain-frequency characteristics of the antenna are shown in Figure 5.9. It is observed from Figure 5.8 that E– and H–plane beam widths lie in the range 138 – 146^o and 124 – 154^o, respectively at the frequency of interest. Table 5.3 shows the radiation pattern characteristics at its resonating frequency of 9.36 GHz. The broadside radiation patterns are achieved in both E– and H– planes over the operating bandwidth of the antenna with fairly low cross-polarized levels in H–plane. The highest cross-polarized lobe levels with corresponding angles of the antenna in E– and H– planes at resonant frequency of antenna is given in Table 5.4. The simulated and measured peak gain values are found to be 6.96 and 6.69 dB at frequencies of 9.49 and 9.36 GHz respectively.

Table 5.3 Radiation pattern characteristics of DS–CDRA at 9.36 GHz.

Parameters		Simulated	Measured
3 dB beam width (degrees)	E– plane	146^o	144^o
	H– plane	130^o	134^o
Front-to-back ratio (dB)	E– plane	12.76	10.78
	H– plane	11.73	11.64

Table 5.4 Highest cross– polarised lobe level with corresponding angle at 9.36 GHz for DS–CDRA.

Parameters		Simulated	Measured
E– plane	Highest cross polar level (dB)	-34.14	-34.29
	Angle (degree)	112 ^{o}	-38^o
H– plane	Highest cross polar level (dB)	-11.81	-10.58
	Angle (degree)	-26^o	-30^o

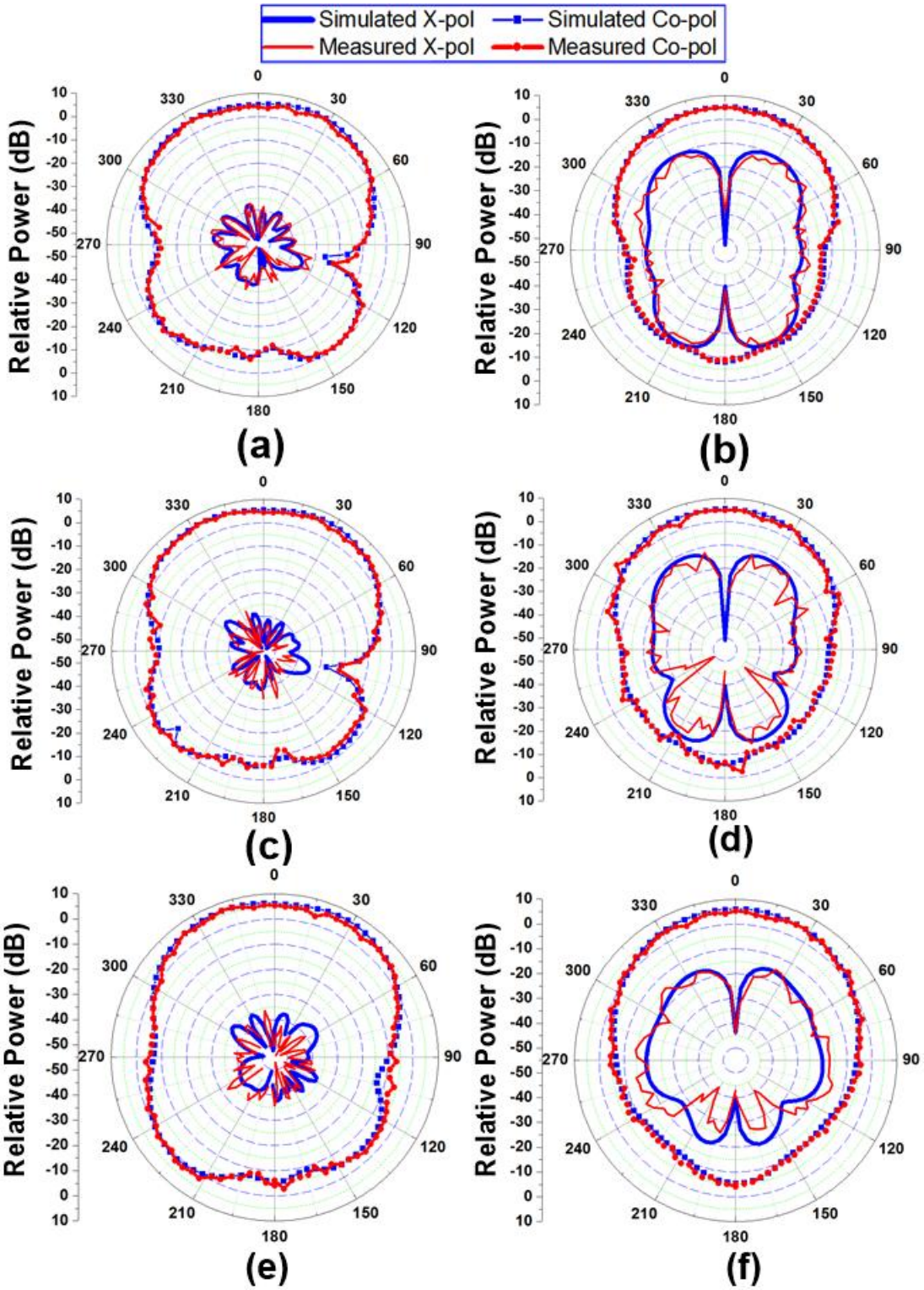

Figure 5.8 Radiation patterns of proposed DS–CDRA at (a) 9.07 GHz [E– plane], (b) 9.07 GHz [H– plane], (c) 9.36 GHz [E– plane], (d) 9.36 GHz [H– plane], (e) 9.76 GHz [E– plane] and (f) 9.76 GHz [H– plane].

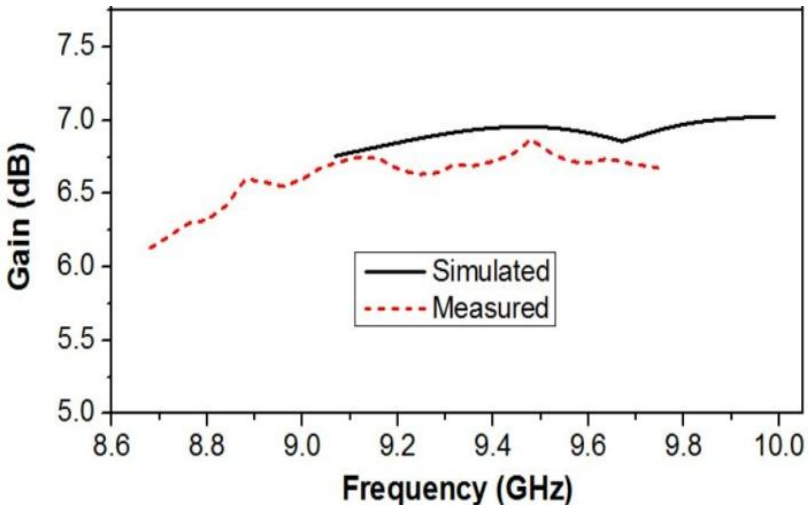

Figure 5.9 Simulated and measured gain – frequency plot of proposed DS–CDRA.

5.4.4 Comparison with other antennas available in literature

Many studies on dielectric resonator antennas (DRAs) using different ε_r values of resonator material have been reported at different frequencies [Kumar and Gupta (2014)]. Mrnka et al. (2016) reported a stacked cylindrical DRA in which resonating element is made by stacking of 14 layers of resonator material with ε_r value of 6.15. Its overall dimensions and other details is given in Table 5.5. It pertains to stacked CDRA but the study was done in C– Band. Their percent impedance bandwidth is much lower than the proposed one [see Table 5.5]. Another study on stacked rectangular dielectric resonator antenna (RDRA) [Tripathi et al. (2015a)] with similar stacking as in proposed DS–CDRA, has also been reported. Its operating frequency range lies in the same band, i.e. X– Band. The percent impedance bandwidth of stacked RDRA reported in literature is lower than the proposed stacked antenna [Table 5.5]. The proposed DS–CDRA provides wide impedance bandwidth of 11.7 % with reasonably good gain of 6.87 dB for X– Band application.

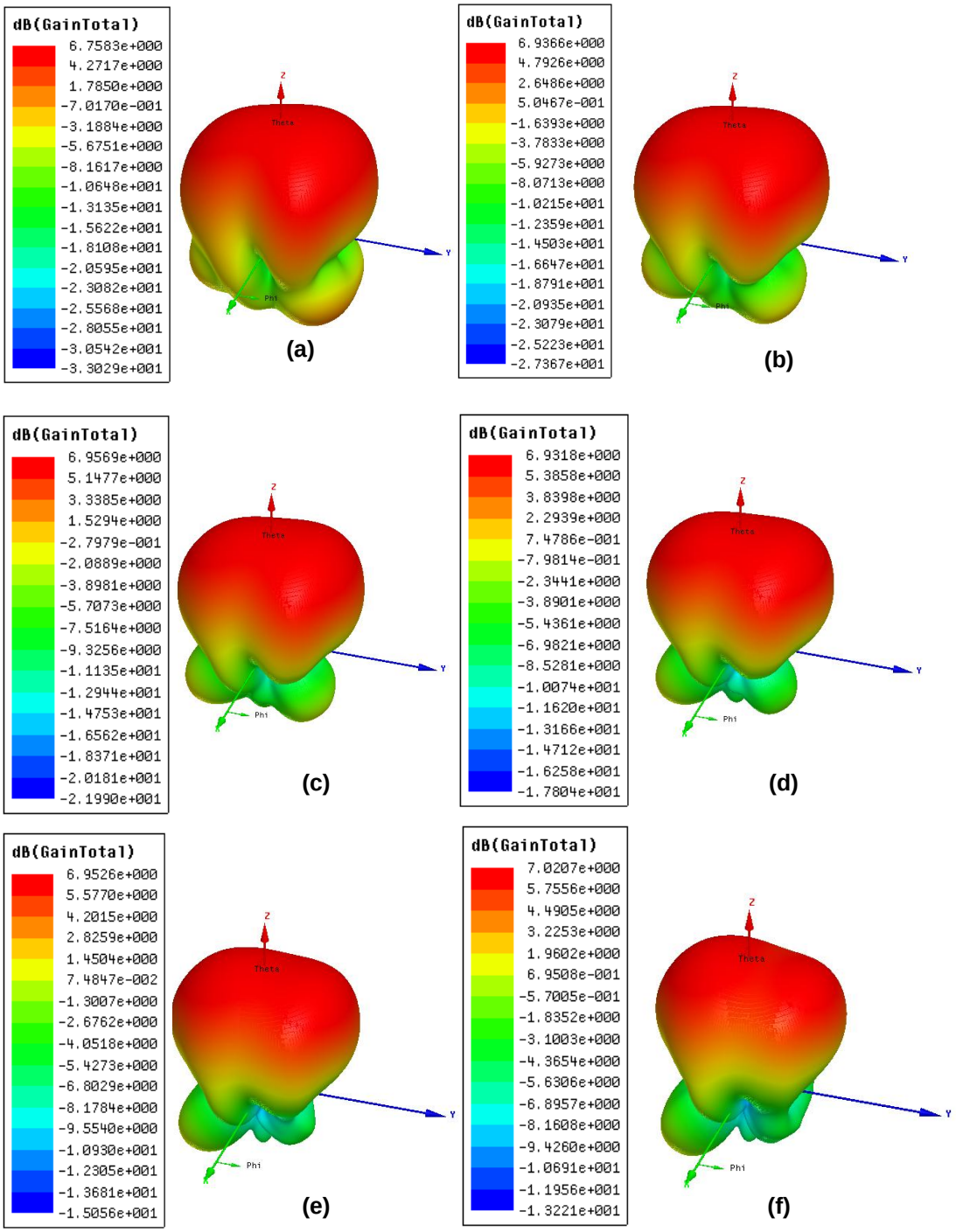

Figure 5.10 3D gain plot of the DS–CDRA at different frequencies (a) 9.08 GHz, (b) 9.36GHz, (c) 9.49 GHz, (d) 9.57 GHz, (e) 9.77 GHz and (f) 9.98 GHz.

Table 5.5 Comparison of different stacked dielectric resonator antenna operating at different frequencies.

DRA shape	ε_r	ε_s	Resonant frequency (GHz)	Excitation	Peak Gain	Physical Dimensions		BW (%)
						a(mm)	h(mm)	
Stacked CDRA [Mrnka et al.(2016)]	6.15	3.4	5.8	Aperture	11.6dB	44.1	22.75	2.6
Stacked RDRA [Tripathi et al. (2015a)]	2.1/27	4.2	9.1	Aperture	6.63dB	10x8^	4.1	7.5
Proposed DS–CDRA	2.1/27	6.2	9.36	Aperture	6.87dB	12	3	**11.71**

ε_r and ε_s: permittivity of DRA resonating material and substrate; a: diameter for cylindrical DRA, ^: Length and width of rectangular DRA; h : height of DRA; BW: Bandwidth

5.5 Summary

In the present work, the LMAP ceramic (x = 0.02) has been used as LTCC substrate for simulation and experimental studies of DS–CDRA. The simulation and experimental results show the favourable radiation patterns. It can be inferred from these results that broadside radiation patterns are obtained in both E– and H– planes at the resonant frequency of the antenna with fairly low cross polar levels in H– plane. The measured results of the fabricated DS–CDRA have been found to be nearly in agreement with corresponding simulation results. The simulated and measured values of gain lie in the ranges 6.76 – 7.02 dB and 6.13 – 6.87 dB respectively over the operating bandwidth of antenna. The proposed antenna can find application in microwave communication, radar and communication systems. It is concluded that the proposed dielectric resonator antennas may find application in radar and radio navigation.